Tracing the impact of former uranium mine sites using stable Pb isotopes: A review

Tingting Geng, Olivier Péron, Arnaud Mangeret, Gilles Montavon, Alkiviadis Gourgiotis

Journal of Environmental Radioactivity 280 (2024) 107547

Contents lists available at ScienceDirect

Journal of Environmental Radioactivity

journal homepage: www.elsevier.com/locate/jenr

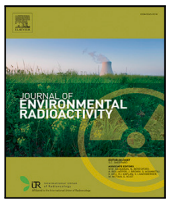

Review

Tracing the impact of former uranium mine sites using stable Pb isotopes: A review

Tingting Geng [a,b], Olivier Péron [a], Arnaud Mangeret [b], Gilles Montavon [a], Alkiviadis Gourgiotis [b,*]

[a] Laboratoire SUBATECH, UMR 6457, IMT Atlantique/Université de Nantes/CNRS/IN2P3, 4, rue Alfred Kastler, Nantes, 44307, France
[b] Institut de Radioprotection et de Sûreté Nucléaire (IRSN), PSE-ENV/SPDR/LT2S, Fontenay-aux-Roses, F-92260, France

ARTICLE INFO

Keywords:
Pollution
U-mine
Lead isotopes
Source tracing
U-mining contamination
Evaluation of environmental impact

ABSTRACT

Tracing pollution originating from uranium (U) mining activities is a key challenge due to the diversity of U sources (geochemical background versus U-ore) and its daughter radionuclides. Among the available tracers that can be used to highlight the impact of these activities on the environment, the application of Pb stable isotopes is relevant. This paper is an overview of the use of Pb isotopes for tracing U-mining impacts due to mining and milling activities. For this purpose, this work outlines the different Pb isotope sources in the environment with a focus on the primary U-rich ores until the mineralized area. This information is an important prerequisite for the understanding of Pb fate during the physical and chemical processing of U-ores. Moreover, an important review regarding the Pb isotope composition of the different types of U mining waste is carried out. Finally, an additional part of analytical procedures including sample preparation and Pb isotopic analysis are also be presented.

Contents

* Corresponding author.
E-mail address: alkiviadis.gourgiotis@irsn.fr (A. Gourgiotis).

https://doi.org/10.1016/j.jenvrad.2024.107547
Received 26 August 2024; Received in revised form 25 September 2024; Accepted 25 September 2024
Available online 17 October 2024

1. Introduction

Uranium (U) mining, which includes the extraction of U ores and subsequent milling processes involving the physical and chemical treatment of U ores to extract uranium, results in the production of the most substantial quantity of radioactive waste. Nowadays, more than 4300 uranium mines worldwide generate 938 × 10^6 m^3 of mill tailings (Abdelouas, 2006). Within the global landscape of U production, the historical extraction of U-ores in France represents a significant undertaking, spanning the years from 1948 to 2001 (IRSN Mimausa, 2023). This extended period of U mining operations included diverse activities such as prospecting, extraction and processing, collectively yielding a substantial production of 76,000 tons of U, accompanied by the generation of approximately 50 million tons (Mt) of mill tailings and 200 Mt of waste rocks dispersed across 250 distinct sites (IRSN Mimausa, 2023). Currently, the sustainable management strategies for these mining materials are grounded on a plan known as the "Plan de Gestion des Matières et Déchets Radioactifs" (PNGMDR) for 2022-2026 (ASN, 2022).

Despite the implementation of comprehensive action plans, natural ecosystems were formerly impacted by U-mining activities, with the record of ancient U-inputs and in certain cases its daughter isotopes, notably ^{230}Th, ^{226}Ra, ^{222}Rn, ^{210}Pb and ^{210}Po in the atmosphere, soils, wetlands, surface and deeper lake sediments (Mangeret et al., 2020; Cuvier et al., 2015; Gourgiotis et al., 2020; Mangeret et al., 2018, 2020; Martin et al., 2020; Stetten, 2018; Stetten et al., 2018; Wang et al., 2013, 2014; Morin et al., 2016; Avasarala et al., 2017). The origin of these inputs is mainly related to the transport of radionuclide-enriched particles by hydraulic and atmospheric transport resulting from mining/milling or rehabilitation activities of U-mining sites or long-term discharges of mine effluents. However, dissolved or colloidal transport can also lead to the dissemination of radionuclides from the mining sites into the environment.

In addition to U-mining impacts, the natural radionuclide inputs due to the weathering and erosion (chemical and/or physical) of local bedrock, such as granite, constitute an additional source of naturally occurring radionuclide contamination. Indeed, high U contents have already been documented in sites non-impacted by U-mining activities (up to 10,000 ppm) (Owen and Otton, 1995), such as Alpine soils (up to 6000 ppm) (Regenspurg et al., 2010; Peña et al., 2020; Lefebvre et al., 2022), as well as ground and surface waters (Owen and Otton, 1995), where the surrounding bedrocks consist mainly of crystalline rocks that commonly contain trace amounts of U. Quantifying the contribution of natural and anthropogenic U and its daughter isotope sources is, therefore, crucial for the determination of the environmental impacts of U-mining activities, which is necessary for guiding and directing waste management strategies and potential remediation actions of U-contaminated sites. In the past, conventional methods, involving the determination of U concentration, or the measurement of the equilibrium state of ^{235}U and ^{238}U decay series were used for identifying U sources (Dickson et al., 1985, 1987; Gulson et al., 1989; Rossman, 1972; Quirt and Benedicto, 2020). Whereas, it is important to recognize that, these methods can help to identify radionuclide "hot spots" but not for tracing the natural and U coming from anthropogenic activities. Acknowledging this challenge, lead (Pb) stable isotopes have been employed for the determination of U sources in the environment for decades (Gulson et al., 1989; Bollhöfer et al., 2006b; Bollhöfer, 2012; Wang et al., 2014). This method offers a robust technique for detecting U-mineralization, frequently proving effective where conventional methods mentioned earlier fell short.

Pb has 4 stable isotopes: ^{204}Pb (1.4%), ^{206}Pb (24.1%), ^{207}Pb (22.1%), ^{208}Pb (52.4%). ^{204}Pb is a primordial isotope and the three last isotopes are the final decay products of natural U and Th decay series (^{238}U → ^{206}Pb, ^{235}U → ^{207}Pb, ^{232}Th → ^{208}Pb). Within U-ores, the presence of high U concentrations results in the production of large quantities of Pb, particularly radiogenic ^{206}Pb and ^{207}Pb. Conversely, a notable depletion in ^{208}Pb is observed, owing to the low concentrations of ^{232}Th. These distinctions give rise to a significant isotopic contrast when compared to natural Pb, which is typically characterized by the predominance of ^{208}Pb.

For the application of stable Pb isotopes in tracing natural U-decay product inputs in the environment, the knowledge of the Pb isotope distribution, (i) from the U-grain scale, at the excavated U-ore, (ii) during its physical and chemical processing (i.e. milling processes) and until (iii) the more distant environmental scale, is crucial.

Numerous studies and review articles focused on the source tracing of anthropogenic inputs by using stable Pb isotopes, thereby enriching the scientific databases of Pb isotopic composition related to various anthropogenic sources. These sources primarily originate from industrial activities, including gasoline, smelting operations, coal combustion, waste incineration (Komárek et al., 2008; Cheema et al., 2020), as well as the extraction and processing of Pb ores (Sangster et al., 2000). Instead, to our knowledge, no scientific review has been prepared to address the application of Pb stable isotopes in tracing the environmental impact of former U-mining inputs. Here, we present an overview of the Pb isotopic source tracing method applied to evaluate the environmental impacts of U-mining activities. We dicussed the mechanisms controlling the migration of radiogenic Pb from its sources, i.e., primary U-enriched minerals at both the nano- and micrometric U-bearing grain scales and the mineralized ore-body scale, and finally to soil and sediments where the signatures are recorded downstream from industrial sites. This helps ensure the correct application of this technique. Finally, an additional section on the main analytical procedures that were used for Pb isotopic analysis was presented.

2. Pb isotopic composition in different materials

2.1. Pb isotopic composition of natural sources

The Pb on Earth consists of primordial Pb and radiogenic Pb. Primordial Pb is the Pb that has existed since the formation of the Earth. The relative abundance and isotopic composition of primordial Pb were initially established through measurements of troilite in iron meteorites dating back to 4.5 billion years ago (Ga) in 1973 (Cumming and Richards, 1975). Among the isotopes of interest, ^{206}Pb, ^{207}Pb, and ^{208}Pb dominate the composition, constituting 18.6%, 20.6%, and 58.9% of primordial Pb, respectively, whereas ^{204}Pb holds a relative abundance of only 2% (Cumming and Richards, 1975). Radiogenic Pb, resulting from the radioactive decay of ^{235}U, ^{238}U, accumulated over time, leading to alterations in the relative abundances of ^{206}Pb, ^{207}Pb, and ^{208}Pb. The growth of radiogenic Pb can be effectively modeled through the application of either a single-stage or two-stage growth curve, which takes into account the initial primordial Pb value and provides estimates of the composition of U, Th, and Pb. In this modeling approach, the Earth is considered to have evolved with relatively uniform values of μ (^{238}U/^{204}Pb) and ω (^{232}Th/^{204}Pb) over the past 3.7 billion years, enabling the estimation of the average Pb isotopic composition of the Earth's crust at various geological ages (Stacey and Kramers, 1975). However, later reassessments led to a refinement of these models, suggesting the direct use of the ^{207}Pb/^{206}Pb ratio for developing a more accurate crustal geochronological model (Cumming and Richards, 1975). An alternative linear increase model to estimate the Present Day Average Crust (PDAC) has been proposed (Cumming and Richards, 1975). These models collectively provide valuable insights into the Pb isotopic composition of the PDAC, as summarized in Table 1. Notably, the ^{206}Pb/^{207}Pb ratio has evolved from its primordial value of 0.9 to approximately 1.20 in the PDAC, while the ^{208}Pb/^{207}Pb ratio has decreased from 2.86 to approximately 2.47 over time.

The Pb isotopic composition of Pb ore minerals tends to remain stable over time, primarily because these ores do not contain significant amounts of the parent isotopes U or Th. Consequently, Pb ores typically exhibit a distinctive low radiogenic Pb signature, characterized by

Table 1
Evolution of Pb isotopic composition for primordial crust and Present Day Average Crust (PDAC).

–	$^{206}Pb/^{204}Pb$	$^{207}Pb/^{204}Pb$	$^{208}Pb/^{204}Pb$	$^{206}Pb/^{207}Pb$	$^{208}Pb/^{207}Pb$	Reference
Primordial	9.3	10.3	29.5	0.9	2.86	Tatsumoto et al. (1973)
PDAC (Two-stage model)	18.70	15.63	38.63	1.20	2.47	Stacey and Kramers (1975)
PDAC (Single-stage model I)	18.47	15.64	38.51	1.18	2.46	Cumming and Richards (1975)
PDAC (Single-stage model II)	18.70	15.63	38.63	1.20	2.47	Cumming and Richards (1975)
PDAC (Linear model)	18.82	15.67	38.89	1.20	2.48	Cumming and Richards (1975)

Table 2
Pb isotopic composition of natural and industrial Pb sources.

Pb source	$^{206}Pb/^{207}Pb$	Reference
Galena (Ranger U mine, Australia)	1.18	Santos and Tassinari (2012)
Galena (Bertholène, France)	1.21	Lévêque (1990)
Leaded gasoline	1.06–1.39	Monna et al. (1997) and Komárek et al. (2008)
Coal combustion	1.13–1.26	Komárek et al. (2008)
Metallurgy activities	1.12–1.18	Komárek et al. (2008)
Waste incineration	1.14–1.25	Komárek et al. (2008)

$^{206}Pb/^{207}Pb$ ratios that generally fall within the range of 1.08 to 1.25 on a global scale (Table 2). This particular type of Pb is often referred to as 'common Pb.' For example, the primary Pb ore galena, sourced from the Ranger mine in Australia and galena from the Bertholène mine in France, both exhibit $^{206}Pb/^{207}Pb$ ratios of 1.18 and 1.21, respectively (Santos and Tassinari, 2012; Lévêque, 1990). The Pb isotopic composition of Pb ore deposits is primarily influenced by three key factors: (i) the initial isotopic composition, (ii) the age of the ore bodies (older Pb ores typically contain more radiogenic Pb than more recent deposits), and (iii) the initial U and Th content within the ores. For a comprehensive overview of the Pb isotopic composition of investigated Pb ore deposits worldwide, a detailed summary table is available in the work by Sangster et al. (2000).

2.2. Pb isotopic composition of non-nuclear industrial sources

Approximately 95% of Pb atmospheric emission arises from anthropogenic activities, which includes a range of sources such as the combustion of leaded gasoline, mining and milling operations, smelting activities, painting factories, and the Pb-acid battery industry (Monna et al., 1999). It is noteworthy that each of these Pb sources exhibits a distinct and characteristic isotopic signature reflecting the Pb isotopic composition of the Pb ores used for production. Table 2 summarizes the Pb isotopic composition of primary anthropogenic Pb sources.

Global investigations of leaded gasoline have revealed a wide range of isotopic compositions, with $^{206}Pb/^{207}Pb$ ratio ranging from 1.06 to 1.39. This variability in isotopic signatures provides valuable insights into the origins of the Pb used in alkyl lead antiknock additives (Komárek et al., 2008). Notably, American leaded gasoline stands out with its significantly elevated $^{206}Pb/^{207}Pb$ ratio, ranging from 1.31 to 1.35 (Doe and Delevaux, 1972). This distinction arises from the use of Pb ores in gasoline production, particularly those sourced from the Mississippi Valley ore deposit, which possesses a unique and more radiogenic Pb isotopic composition. In contrast, the Pb ores commonly used in Australia, from the Broken Hill deposit, is characterized by an extremely low $^{206}Pb/^{207}Pb$ ratio (1.03–1.10). Investigations of the Pb isotopic composition of other industrial sources, including coal combustion, metallurgical activities, waste incineration, and mining activities have been undertaken (Table 2). Particularly, the U-mining materials show a Pb isotopic signature, known as 'radiogenic Pb signature', which differs from other sources due to the high ^{206}Pb and ^{207}Pb content compared to that of ^{208}Pb.

2.3. Radiogenic Pb signature in the U-mining industry

2.3.1. Major U-rich mineral phases

U-ore minerals.

U is commonly found in the form of accessory minerals in nature, which constitutes a minor portion of bedrock. Depending on the geological conditions, a diverse range of primary and secondary U minerals were precipitated from U-bearing fluids via mechanisms such as adsorption, reduction–oxidation, and microbial activity in the form of U (IV) or U(VI) (Langmuir, 1978; Fayek et al., 2011). Some of the most common U-ore minerals are uraninite, pitchblende, and coffinite (Fayek et al., 2011). Among them, primary U mineral uraninite and pitchblende represent the initial form of U deposition, while secondary minerals arise as alteration products of uraninite under reducing conditions including autunite, coffinite, uranophane, and torbernite. These minerals are often identified in U deposits.

Uraninite (UO_2) occurs in crystalline form and can be found in various crystallographic shapes. It can either exist as a primary constituent within granitic rocks and pegmatites or as a secondary mineral associated with Ag, Pb, or Cu ores (Dana et al., 1985). Pitchblende is an amorphous variety of uraninite. It also primarily contains uranium dioxide, but in varying proportions. Pitchblende occurs as fine-grained aggregates and is poorly crystalline, typically precipitating in environments characterized by lower temperatures than uraninite, and usually contains less thorium (Th) and rare earth elements (REE) (Dahlkamp, 2013; Janeczek et al., 1996). Uraninite and pitchblende hold a distinguished status as the predominant U-ore minerals, both in terms of their abundance in the Earth's crust and its substantial economic significance (Burns and Finch, 2018) on a global scale. Coffinite represents the second most prevalent U-ore mineral and is a major U-bearing phase found in numerous sandstone-hosted U deposits (Burns and Finch, 2018).

In the natural environment, pure UO_2 is rare, as it contains cation impurities, including but not limited to Pb, Ti, Fe, Si, Th, Zr, REE, Ca (Burns and Finch, 2018). The formation of alteration products (secondary U-ore minerals) mentioned earlier, which originate from uraninite, is directly connected to the presence of these impurities and the chemical compositions of the fluids involved in the alteration process (Janeczek and Ewing, 1992, 1995). Among these impurities, radiogenic Pb is the most important impurity in geologically old uraninite samples due to the radioactive decay of U. Remarkably, the concentration of radiogenic Pb in uraninite can be exceptionally high, reaching levels of up to 15–20 wt% in the form of PbO (Berman, 1957; Janeczek and Ewing, 1991, 1992, 1995).

In contrast to the previously mentioned Pb sources, U-ore mineral phases exhibit a distinct Pb isotopic composition characterized by high $^{206}Pb/^{207}Pb$ ratios and low $^{208}Pb/^{207}Pb$ ratios, attributed to the radioactive decay of ^{238}U and ^{235}U within these mineral phases. The investigations of the radiogenic Pb signature of U-rich minerals including uraninite, pitchblende, torbernite, and autunite on a global scale is summarized in Table 3. The radiogenic Pb signature within U-ores can display significant variability, even within the same type of mineral. The torbernite of Urgeiriça mine (Portugal) shows the most radiogenic signature with a $^{206}Pb/^{207}Pb$ ratio around 20. Pitchblende from the Ranger U mine in Northern Australia exhibits a $^{206}Pb/^{207}Pb$ ratio as high as 12.73, while pitchblende from Portugal shows a $^{206}Pb/^{207}Pb$ ratio of approximately 1.91 (Table 3). This divergence in Pb isotopic ratios among U-ore minerals cannot be solely attributed to the age of the U-ore deposits; it is also related to variations in U and Th concentrations and the initial Pb isotopic composition present in these minerals.

The radiogenic Pb contained within uraninite assumed the Pb(II) state, effectively replacing U(IV) within the crystal lattice (Syverson et al., 2019). However, Pb(II) possesses a larger ionic radius of 0.129 nm for a coordination number of VIII, exceeding the ionic radius (0.100 nm) of U(IV) with the same coordination number. Consequently, Pb cannot directly substitute for U within the uraninite structure. Instead, the radiogenic Pb is expelled from uraninite, leading to the formation of a monolayer of amorphous massikote (PbO) (Janeczek et al., 1996).

The migration of radiogenic Pb has been well-documented in various studies. For instance, at Shea Creek in Saskatchewan, Canada, 53% to 64% radiogenic Pb in uraninite was found to migrate over considerable distances, reaching up to 700 meters away from the ore body and trapped within galena (Kister et al., 2004). Recent leaching tests on Olympic Dam uraninite confirmed the mobility of Pb. In these tests, ^{206}Pb and ^{238}U were primarily localized at the surface or in large pores/grain boundaries within uraninite (Ram et al., 2021). In terms of metamorphism and alteration history, radiogenic Pb within uraninite could be released from the crystal lattice when there were changes in the oxidation state of the metasomatic hydrothermal fluid. During this process, U(IV) within uraninite mobilized into soluble U(VI) species through oxidative dissolution. This behavior was mainly attributed to the fact that the solubility of Pb(II) in hydrothermal fluids was less sensitive to changes in the fluid's redox conditions compared to U-bearing minerals. Instead, it was primarily influenced by factors such as temperature and the concentration of dissolved ligands, including associations with chloride and sulfide ions (Etschmann et al., 2018). Depending on changes in hydrothermal fluid chemistry, Pb became susceptible to mobilization through various mechanisms of U-bearing mineral alteration, such as dissolution–reprecipitation and/or mineral replacement. Janeczek and Ewing (1995) also documented the release of radiogenic Pb from uraninite in the natural reactors of Oklo, Gabon. They proposed several mechanisms for this release, including episodic and thermally activated processes like mineral dissolution, grain boundary diffusion, exsolution via continuous precipitation, volume diffusion, and co-transport of intermediate daughter products from uraninite. A more recent study on Oklo uraninite reactor zone samples suggested that multiple events involving fluid interactions and internal UO_2 recrystallization caused the loss of incompatible elements like Pb. These elements were sequestered from the UO_2 matrix into their mineral phases (Evins et al., 2005).

Coffinization, resulting in the transformation of uraninite into coffinite, represents another mechanism leading to the release of Pb, particularly the radiogenic Pb. Several studies indicate that during the process of uraninite alteration, the actual loss of Pb can be as high as 100%. In the partially altered zones of uraninite, known as coffinization, grains exhibit diminished levels of radiogenic Pb compared to the surrounding primary, unaltered zones of uraninite (Janeczek and Ewing, 1995; Alexandre and Kyser, 2005; MacMillan, 2016). Similarly, for brannerite, preferential retention of radiogenic Pb in the altered brannerite was also observed and attributed to Pb serving as a network modifier within the Ti-Si-O framework of the glass-like structure of metamict brannerite (Rollog et al., 2019).

It is important to highlight that these migrations of radiogenic Pb do not significantly alter the isotopic composition of Pb in uraninite. This lacks of preferential release of specific Pb isotopes results in no significant isotopic fractionations.

Other U-rich mineral phases.

Mineral phases such as titanite, zircon, and monazite consistently incorporate minor quantities of U, resulting in a radiogenic Pb signature. They are typically accessory minerals that occur alongside U-bearing minerals in U-ore deposits as accessory minerals or gangue minerals. During the formation, they tend to concentrate on U and Th while rejecting Pb, which minimizes the common Pb. Consequently, the majority of the Pb found within zircons is produced in situ through radioactive decay processes (Syverson et al., 2019; Watson et al., 1997).

Zircon and titanite contain trace amounts of U, usually constituting less than 1 wt%, which subsequently leads to the generation of radiogenic Pb. Investigations have shown that this Pb is primarily present in the form of nano-scale inclusions (Kusiak et al., 2015) or as a substitution for Zr/Ti at concentrations below 1 wt% (Kogawa et al., 2012). Moreover, it is noteworthy that Pb and U distributions within these two minerals are often decoupled at both the μm and nm scales (Kogawa et al., 2012; Kirkland et al., 2018).

2.3.2. U concentrates

The U-ore concentrate, commonly referred to as "yellow cake", is the end product of U-mining activities. It is obtained through a series of physical and chemical processing steps applied to uranium ores. Yellow cake can also be recovered as a byproduct during the extraction of other materials, such as copper and gold.

Pb isotopic fractionation is generally considered negligible during the processing of U-ores. As a result, the Pb isotopic composition in U-ore concentrates is expected to be close to that of the original raw U-ore. The Pb isotopic composition of investigated yellow cake varies from 1.21–9.73 (Varga et al., 2009; Švedkauskaite-LeGore et al., 2007). However, there have been instances where significant variability in Pb isotopic composition has been observed between U-ore and yellow cake samples originating from the same mine. In some cases, this variability can be as high as a factor of four, particularly in the $^{208}Pb/^{206}Pb$ ratios. This variation can be attributed to the chemical purification processes involved in U-ore processing. These processes result in the continuous separation of radiogenic Pb (and other impurities) from the U-ore, gradually replacing it with natural Pb found in the chemical reagents as an impurity (Švedkauskaite-LeGore et al., 2007; Varga et al., 2009).

2.3.3. U tailings

The investigation of Pb isotopic composition within U-tailings generated by U-mining activities remains somewhat limited in the existing literature. The Pb isotopic composition of these investigated U-mill tailings are summarized in Table 4. Notably, data on Pb isotopic composition have primarily been obtained from mill tailings of France, Gabon and Portugal (Santos and Tassinari, 2012; Beaumais et al., 2022), with $^{206}Pb/^{207}Pb$ ratio ranging from 1.545–7.157. These U mill tailings exhibit a clear radiogenic signature similar to that of U-ores. Two additional studies have expanded upon this dataset, focusing on the Pb isotopic composition of bulk mill tailing samples. These samples were specifically employed as endmembers in environmental assessments in Canada and China, respectively (Dang et al., 2018; Liu et al., 2018). Additionally, one study gathered Pb isotopic data from particles retained in filtered water samples obtained from a borehole within a U mill tailing dam (Gulson et al., 1989). However, the Pb isotopic composition determined in U mill tailings cannot accurately represent the true radiogenic Pb composition of U ores, even though

Table 3
Pb isotopic composition of U-rich minerals.

Location	Sample	$^{206}Pb/^{207}Pb$	$^{208}Pb/^{207}Pb$	Reference
Australia	Uraninite (Koongarra)	13.04	0.018	Isobe et al. (1997)
Australia	Unknown U-ore (Olympic dam)	8.33 ± 0.31	1.44 ± 0.07	Švedkauskaite-LeGore et al. (2007)
Australia	Unknown U-ore (Ranger mine)	9.16 ± 0.43	0.14 ± 0.07	Švedkauskaite-LeGore et al. (2007)
Portugal	Pitchblende	1.914 ± 0.003	2.363	Santos and Tassinari (2012)
Australia	Alligator Rivers pitchblende	Up to 12.73	<0.01	Hills and Richards (1976)
Finland	Coffinite	2.06 ± 0.29	2.49 ± 0.35	Pomiès et al. (2004)
Portugal	Torbernite	19.816 ± 0.064	0.079	Santos and Tassinari (2012)
Portugal	Autunite	18.773 ± 0.026	0.113	Santos and Tassinari (2012)
Australia	Uranyl minerals	12.722	0.047	Isobe et al. (1997)

Table 4
Pb isotopic composition of U mill tailings.

Location	Sample	$^{206}Pb/^{207}Pb$ $\pm 2\sigma$	$^{208}Pb/^{207}Pb$ $\pm 2\sigma$	Reference
Portugal	Urgeiriça mine	1.545 ± 0.004	2.43 ± 0.02	Santos and Tassinari (2012)
France	Le Bosc (Lodève)	2.25 ± 0.02	2.33 ± 0.01	Beaumais et al. (2022)
France	L'Ecarpière	5.812 ± 0.049	1.871 ± 0.009	Beaumais et al. (2022)
France	Bellezane	1.862 ± 0.007	2.388 ± 0.005	Beaumais et al. (2022)
France	Le Bernardan (Jouac)	5.924 ± 0.084	1.856 ± 0.009	Beaumais et al. (2022)
Gabon	Mounana	7.157 ± 0.082	0.222 ± 0.001	Beaumais et al. (2022)
Chine	Shaoguan	1.946	2.378	Liu et al. (2018)
Canada	Bow Lake(Madawaska Mine)	9.13 ± 0.04[a]	2.62 ± 0.01[a]	Dang et al. (2018)
Australia	Ranger mine tailings dam water particles	10	0.049	Gulson et al. (1989)

[a] Unknown coverage factor (2σ).

the Pb isotopic composition of French U mill tailings exhibits a clear radiogenic signature similar to that of U ores, confirming the preservation of the original Pb isotope characteristics of U ores (Beaumais et al., 2022). It is essential to note that the Pb isotopes identified in U mill tailings are a mixture of Pb originating from two distinct sources: (i) common Pb, which may originate from either the U-ore host rock or the reagents employed during U extraction, and (ii) radiogenic Pb from U ores.

SEM-EDX observations revealed that phases hosting radiogenic Pb include both U-rich and U-free S-rich phases. Specifically, the radiogenic Pb is primarily hosted within primary U-rich phases that persist after the milling process. Additionally, radiogenic Pb is also encountered in U-free S-rich phases, which could potentially originate from either (i) residual Pb-sulfide (galena) associated with the natural hydrothermal alteration of U-rich phases or (ii) newly formed Pb-Ba-Ra sulfate resulting from the milling process involving sulfuric acid (Beaumais et al., 2022).

3. Using Pb isotopic composition for U-mine environmental impact assessment

3.1. Pb isotopic composition in U-mine impacted environmental samples

In the field of environmental sciences, Pb isotopic compositions are typically expressed as ratios, including $^{206}Pb/^{204}Pb$, $^{206}Pb/^{207}Pb$, $^{208}Pb/^{207}Pb$, and more. Notably, $^{206}Pb/^{207}Pb$ and $^{208}Pb/^{207}Pb$ ratios hold particular importance due to their relative abundances and pronounced variability across diverse sources (Komárek et al., 2008; Cheema et al., 2020; Bird, 2011).

Pb isotopes have been considered a relevant geochemical tracer for identifying the sources of Pb in various media since the 1960s (Chow and Patterson, 1962). They were also used for the exploitation of Pb ore deposits and the subsequent release of this Pb into the environment (Bird, 2011). The application of Pb fingerprinting for the detection of U deposits can be dated back to 1985 (Dickson et al., 1985). In this pioneering study, it was demonstrated that the $^{206}Pb/^{204}Pb$ ratio can identify U deposits, even in regions characterized by low U concentrations where other conventional techniques may fall short (Dickson et al., 1985). This early use of Pb fingerprinting marked a significant breakthrough in the field of U-deposit exploration, emphasizing the unique capabilities of Pb-stable isotopes in geochemical research. Following this work, Pb stable isotopes have been extensively employed in tracing the origins of U-rich materials, including U ores, U concentrates, U tailings, and U-impacted samples (Santos and Tassinari, 2012; Keegan et al., 2008; Varga et al., 2009).

In the field of environmental science, high concentrations of U and various daughter radionuclides have been frequently documented in diverse environmental compartments. These include soils, sediments, vegetation, and notably, wetlands, which often serve as significant sinks for these elements. Such accumulations can arise from natural weathering and erosion processes, as well as the discharge of materials from U mining activities. To determine the source of these radioactive contaminants, number of works have turned to the use of Pb isotope ratios in combination with elemental analyses. This integrated approach has proven valuable in tracing the origins of contamination (Dang et al., 2018; Martin et al., 2020; Bollhöfer et al., 2006a; Bollhöfer, 2012; Gourgiotis et al., 2020; Frostick et al., 2008, 2011; Coetzee and Rademeyer, 2006; Liu et al., 2018; Cuvier et al., 2016; Geng et al., 2024; Wang et al., 2024). The Pb in the U-contaminated environmental samples is a mixing of natural Pb (common Pb) and uranogenic Pb (radiogenic Pb). However, they still exhibit an enrichment of radiogenic Pb isotopes (^{206}Pb and ^{207}Pb), indicative of U-rich materials produced during mining activities. The isotopic compositions of samples impacted by U mining activities are summarized in Table 5.

While the radiogenic Pb signature in environmental samples may not reach the same levels as those observed in U ores, U concentrates, and U tailings, this enrichment still enables the differentiation between U ore sources and common Pb in geogenic sources, which typically displays a ratio around 1.1–1.2. The application of this technique to environmental samples collected from U-mine contaminated areas has provided valuable insights into the dispersion of U from former U mine sites into the surrounding environment, driven by various mechanisms including hydraulic and aeolian transport.

This dispersion is particularly pronounced in the downstream area. The Pb isotopic composition of samples collected downstream exhibits variations that correspond to different lithologies and often displays a mixed signature influenced by heavy minerals like monazites originating from bedrock erosion, natural dust, clays, silts, and industrial Pb sources (Bollhöfer, 2012; Frostick et al., 2011). Then, a noticeable decrease in the $^{206}Pb/^{207}Pb$ ratio was observed in samples collected upstream as the distance from the mining site increased, eventually

Table 5
Pb isotopic composition of U-mine contaminated samples.

Location	Sample	$^{206}Pb/^{207}Pb$[a]	$^{208}Pb/^{207}Pb$[a]	Reference
Canada	Soils and lake sediments	1.17–4.13	2.23–2.28	Dang et al. (2018)
Australia	Aerosol particles	1.58–4	1.55–2.26	Bollhöfer et al. (2006a)
Australia	Downstream sediments	1.26–2.20	2.30- 2.68	Santos and Tassinari (2012)
Australia	Downstream mussels	1.21–2.35	2.23–2.49	Bollhöfer (2012)
Australia	Surface sediments along drainage channels	8.72–8.92	0.26–0.31	Frostick et al. (2011)
Australia (Koongarra)	Surface sediments within U mineral lease	1.51–1.8	2.52–2.63	Frostick et al. (2011)
Australia (Nabarlek)	Soil scrapes from catchment	1.62–3.11	2.32–2.70	Frostick et al. (2011)
Australia	Upstream sediment (depth < 0.3 m)	1.32	2.66	Munksgaard et al. (2003)
Australia	Upstream sediment	1.25[b]	2.53[b]	Munksgaard et al. (2003)
Australia	Estuaire sediment	1.25[b]	2.53[b]	Munksgaard et al. (2003)
China	Surface sediment from the recipient stream of U mining waste	1.25–1.87	2.39–2.48	Liu et al. (2018)
China	Sediments from the U mine downstream natural water reservoir	1.25–1.58	2.43–2.48	Liu et al. (2018)
China	Surface sediments and soil near a uranium hydrometallurgical site	1.218–1.669	–	Wang et al. (2024)
Portugal	Suspension particles around the tailing deposits	1.65 ± 0.01	2.41 ± 0.07	Santos and Tassinari (2012)
Portugal	Colloidal phases in water cores	1.67 ± 0.01	2.32 ± 0.05	Santos and Tassinari (2012)
France	Contaminated surface soil	1.520 ± 0.001	2.462 ± 0.003	Cuvier et al. (2016)
France	Downstream river sediment	1.226 ± 0.001	2.468 ± 0.003	Cuvier et al. (2016)
France	Downstream soils and sediments of the mine water outlet	1.27–10.73	1.12–2.45	Gourgiotis et al. (2020)
France	Soil and sediments of downstream wetland	1.24–1.64	2.41–2.48	Martin et al. (2020) and Geng et al. (2024)
South Africa	River sediments of the Wonderfonteinspruit	1.70–4.60	1.23–2.19	Coetzee and Rademeyer (2006)

[a] The uncertainty is 2σ.
[b] The mean value of 53 samples.

converged towards geological background values (~1.2) (Liu et al., 2018). This trend underscores the potential dispersion of U and other daughter nuclides via hydraulic transport. The presence of radiogenic Pb signatures in samples collected from downstream wetlands of former U mines (Gourgiotis et al., 2020; Martin et al., 2021; Cuvier et al., 2016; Liu et al., 2018), as well as in groundwater (Vecchia et al., 2017), suspension materials, and bioindicators (Bollhöfer et al., 2006a) such as mussels near former U mine areas, further supports the dispersion of U-rich particles from tailing deposits downstream area via hydraulic transport.

On the other hand, eolian transport has also been identified as a significant mechanism for the dispersion of U-mining particles. Surprisingly, the ^{206}Pb and ^{207}Pb ratios of dust and leaves collected on trees located up to 200 km away from the pit center reach values as high as 8.5, which is comparable to the ratios observed in particles from tailings dam water. However, a positive correlation between the Pb fingerprint and the distance from the mine site still exists. Seasonal variations in Pb isotopic composition have also been observed, exhibiting a contrasting trend with rainfall patterns. This phenomenon is attributed to the effective reduction in dust generation during the wet season (Bollhöfer et al., 2006a). These findings suggest that drier and less regulated environments may facilitate the dispersion of U in the form of aerosols over greater distances from the U mine area.

3.2. Assessing the U-mining impact: Quantification of radiogenic Pb

A three-isotope plot (^{206}Pb, ^{207}Pb, ^{208}Pb) is commonly employed to visually illustrate the sources contributing to the Pb isotopic composition of samples (Dang et al., 2018; Martin et al., 2020; Bollhöfer et al., 2006a; Bollhöfer, 2012; Gourgiotis et al., 2020; Santos and Tassinari, 2012; Frostick et al., 2008; Varga et al., 2009; Liu et al., 2018; Cuvier et al., 2016). Typically, most studies have employed a binary mixing model, assuming that the Pb in their environmental samples is a mixture of two primary sources: (i) geogenic Pb derived from the local geochemical background, and (ii) uranogenic Pb originating from U mining activities. These two sources are treated as end-members, and the Pb isotopic ratios of the samples when plotted on the three-isotope plot ($^{206}Pb/^{207}Pb$ vs $^{208}Pb/^{207}Pb$), align along a characteristic mixing line that illustrates the contributions of these two end-members. As shown in Fig. 1, the Pb present in the tailings and the U-contaminated soils and sediments is a mixture originating from two primary sources: U-rich minerals such as pitchblende, and the local geochemical background (PDAC). Other potential Pb sources, including leaded gasoline and industrial emissions, do not align with them.

The binary model is also useful for quantifying the contribution of U mining to environmental samples in the U-contaminated area, which refers to the proportion of Pb originating from U mines in the total Pb composition. The most commonly used equation for quantifying this impact is as follows (Eq. (1)) (Bollhöfer et al., 2006a; Bollhöfer, 2012; Frostick et al., 2008, 2011; Liu et al., 2018):

$$\left(\frac{^{206}Pb}{^{207}Pb}\right)_{\text{samples}} = f * \left(\frac{^{206}Pb}{^{207}Pb}\right)_{\text{mine}} + (1-f) * \left(\frac{^{206}Pb}{^{207}Pb}\right)_{\text{background}} \quad (1)$$

In most publications, the factor "f" is assumed to represent the proportion of radiogenic Pb to the total Pb content in the samples. Bollhöfer et al. (2006a) employed the mixing model, considering the global aerosol Pb isotopic ratio ($^{206}Pb/^{207}Pb = 1.15$) as the background end member and the filtered particles from the tailing dam ($^{206}Pb/^{207}Pb = 9.69$) of Ranger mine in Australia as the uranogenic Pb end member. Using this approach, the contribution of the Ranger mine to the total Pb content in airbone particles was estimated within the Jabiru East region (2.5 km northwest of the mine), 13% respectively. This estimation aligns with their previous study within the same U mining region, which showed that uranogenic Pb input accounted for 10% of the Pb in mussels (Bollhöfer, 2012). Additionally, Cuvier et al. (2016) inferred that approximately 26% of the Pb in U-contaminated soil originated from U mining activities, specifically the Bertholène mine in France.

However, it is crucial to delve deeper into the nuances of the factor "f" calculated using Eq. (1). Conventional usage of this factor defines it as the fraction of radiogenic ^{207}Pb (not the total radiogenic Pb) originating from the uranium mine relative to the total ^{207}Pb content (common and radiogenic Pb) in the samples. Indeed, while this conventional interpretation is valid, it provides a somewhat limited perspective that may lead to underestimating the true impact of U-mining by up to 35% (Gourgiotis et al., 2020). This limitation arises from the fact that this estimation considers only ^{207}Pb. To obtain a more accurate assessment, it is essential to account for all Pb isotopes. This requires evaluating the abundance of total Pb (common and radiogenic).

In response to this challenge, an alternative equation has been proposed (Eq. (2)), which takes into account the isotopic abundance,

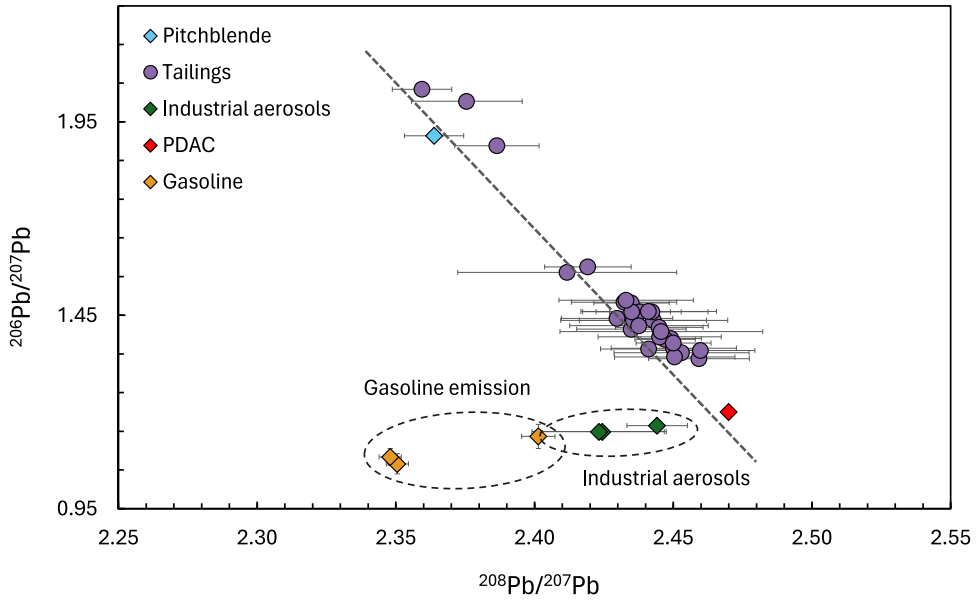

Fig. 1. The binary mixing model with tailing samples (data from Santos and Tassinari (2012)); environmental soil and sediment samples contaminated by U-mining activities, data from Geng et al. (2024), U mineral-pitchblende, and Pb sources including leaded gasoline emission, industrial aerosols (Monna et al., 1999).

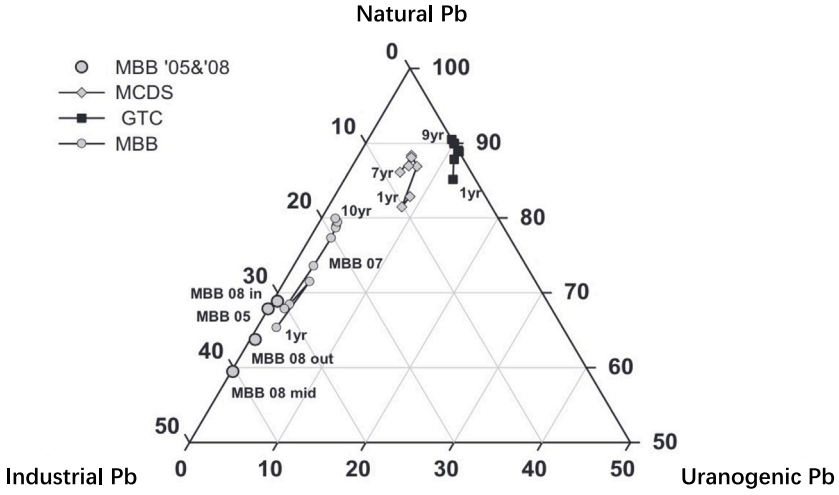

Fig. 2. Ternary mixing model for various Pb sources contribution to the total Pb concentration in mussels from Georgetown Creek (GTC), Magela Creek downstream (MCDS) and Mudginberri Billabong (MBB), downstream of Ranger mine in Australia (Bollhöfer, 2012). Samples from Mudginberri Billabon were collected in 2005 and 2008. The age of mussels were also shown in this figure.

providing a more precise and robust assessment of the environmental impact of U-mining (Gourgiotis et al., 2020).

$$Ab^{206}_{sample} = k * Ab^{206}_{mine} + (1-k) * Ab^{206}_{background} \quad (2)$$

It has also been observed that when the sample point deviates from this binary mixing line (Fig. 1), it indicates the influence of additional Pb sources, such as potential industrial input or leaded gasoline, which typically exhibit a low $^{206}Pb/^{207}Pb$ ratio. When a third Pb source comes into play, a ternary mixing model becomes applicable. In such cases, knowing the isotope ratios of the sources, the relative contributions of each pair of sources need to be calculated. For example, Bollhöfer (2012) identified the impact of industrial emissions on young mussels inhabiting Mudginberri Billabong, a channel billabong located 12 km downstream from the Ranger U mine in Australia (Fig. 2).

It is important to note that the contribution of uranogenic Pb to environmental samples can be equal to that of U-mining input originating from mining activities only when there is a simultaneous dispersion of both U-Pb dispersions.

4. Analysis methods of Pb isotopes

4.1. Sample preparation

Studies in U-mining areas have investigated various samples such as soils and sediments (Martin et al., 2020; Cuvier et al., 2016; Gourgiotis et al., 2020), leaves (Bollhöfer et al., 2006a), water (Vecchia et al., 2017), mussels (Bollhöfer, 2012), etc. Prior to analysis, sample preparation is an essential procedure for reliable and precise measurements. Various digestion and Pb extraction protocols have been employed, such as aqua regia digestion (Vecchia et al., 2017), HF/HNO_3 mixture digestion (Santos and Tassinari, 2012), micro-oven digestion, ethylenediaminetetraacetic acid (EDTA) extraction (Komárek et al., 2006), and total digestion (using HF–HNO_3–HCl–$HClO_4$) (Komárek et al., 2006), etc. The selection of the digestion/extraction method for samples should not only align with the specific research objectives but also take into account the physical and chemical properties of the samples, especially for soil samples. Nearly no significant differences

Table 6
The chemical separation protocol of Pb isotopes.

Steps	Manhes et al. (1984)	Tanimizu and Ishikawa (2006)	Millet (2007)	Kuritani and Nakamura (2002)	Koide and Nakamura (1990)
Sample mass (mg)	100	–(0.02–0.04 mg Pb)	500	–	100
Resin	Merck AG 1X8 70–150 mesh	Bio-Rad AG 1-X8 (200–400 mesh)	AG 1X8	Bio-Rad AG-1X8	Biorad AG1-X8
Resin volume (μL)	15	100	10	100	30
Pre-washing of column (mL)	0.5M HBr (1)/H_2O (0.1)/0.5M HON_3 (1)/H_2O (0.1)	0.2M HCl (3 mL)	0.5M HON_3 (1.5)/H_2O (1.5)		
Conditioning	0.5M HBr (0.1)	–	0.8M HBr (0.5)	0.5M HBr (0.3)	
Sample introduction (mL)	–	–	12	1	
Matrix elution (mL)	0.5M HBr (2)	Mixed acid of 0.25M HBr+0.5M HON_3 (2.5)	0.8M HBr (0.5)	Mixed acid of 0.25M HBr+0.5M HON_3 (2.5)	0.5M HBr (0.3)
Pb elution (mL)	H_2O (0.5)	H_2O (1)	0.2M HCl (1)	H_2O (1)	H_2O (0.75)

in Pb isotopic composition were observed among different digestion methods for surface soil samples containing high soil organic matter content (Komárek et al., 2006). However, for mineral horizons of this soil samples, the total digested samples show the highest $^{206}Pb/^{207}Pb$ ratios while the EDTA extracts from mineral soil samples display the lowest $^{206}Pb/^{207}Pb$ ratios (Komárek et al., 2006). These differences between digestion/extraction method can be attributed to the existence of two different Pb pools: one weakly bound and another strongly bound. In this case, using combination of total digestion methods and extraction methods (targeting labile Pb fraction) seems optimal for result interpretation (Komárek et al., 2008).

Considering the potential presence of common Pb in airborne dust, and in experimental materials such as laboratory tubes, and reagents, a pre-cleaning of all experimental materials is suggested. Moreover, the use of ultrapure reagents, dedicated chemistry banks, and sample preparation under a controlled laminar flow environment is highly recommended in order to minimize external contamination and ensure the accuracy of the measured Pb isotopic signature.

Additionally, Pb purification is essential to separate Pb isotopes from matrix elements. This step holds particular significance due to the potential influence of minor matrix elements, such as Zn or Cd, which can adversely affect the ionization efficiency of analytical instruments (Woodhead et al., 1995). It is also crucial to minimize the risk of spectral (polyatomic and isobaric) and nonspectral interference, ensuring the accuracy of Pb isotopic analysis, particularly the main isobaric interference of ^{204}Hg on ^{204}Pb.

The most widely employed methods of purifying Pb from a matrix operate by passing the dissolved sample over an anion exchange resin and two methods are mainly employed to elucidate Pb from resin: HBr-HCl method and HBr-HNO_3 method (Kamber and Gladu, 2009; Manhes et al., 1984). The dilute HBr is employed to efficiently eliminate the major element matrix from nearly all geological materials, except sphalerite ((Zn, Fe)S) while holding the Pb on the resin. The subsequent Pb elution from resin involves the use of dilute HNO_3 or HCl. A comparison was carried out between these two methods, revealing that although HNO_3 exhibited a slight advantage in terms of blank quality and yield, the HCl method stands out in significantly superior matrix removal capabilities (Kamber and Gladu, 2009). Detailed protocols employed in previous Pb analyses are summarized in Table 6.

4.2. Mass spectrometry analysis

Recent progresses in analytical techniques have greatly facilitated the use of Pb isotopes as geochemical tracers. Mass spectrometry is an analytical technique that serves as a powerful tool for determining Pb isotopic ratio. According to the ion source, two primary approaches have been employed: thermal ionization mass spectrometry (TIMS) and inductively coupled plasma mass spectrometry (ICP-MS).

Table 7
Summary of analytical precision for Pb isotope determinations by different analytical techniques (Bird, 2011).

Technique	Relative Standard Deviation (RSD %)
TIMS	0.001–0.01
ICP-MS quadripole	≥0.1
HR/MS-ICP-MS	≤0.1
MC-ICP-MS	≤0.002–0.02

TIMS was the only method to measure accurately Pb isotope ratios before the invention of ICP-MS. It provided reliable measurements with high precision and accuracy in environmental samples (Weiss et al., 1999; Ghazi and Millette, 2005). The relative standard deviation (RSD) ranges from 0.001% to 0.1% (Komárek et al., 2008; Bird, 2011; Cheng and Hu, 2010).

Inductively Coupled Plasma Mass Spectrometry (ICP-MS) has been widely employed in recent years, marking a notable shift in determining Pb isotopic ratios in the field of geochemical studies. The Pb isotope analysis by ICP-MS was first introduced in environmental sciences in 1991 (Hopper et al., 1991). Compared to TIMS, ICP-MS offers efficient ionization of almost all elements, rendering it particularly advantageous for elements that pose challenges in ionization in TIMS (Albarède and Beard, 2004). The higher processing speed of the sample preparation process leads to a substantial reduction in the time and effort required compared to traditional methods. This technique also enables a higher sample throughput, allowing for more efficient data collection and analysis (Quétel et al., 1997). However, it is important to note that the precision and accuracy of the data obtained using this method is limited, ranging from 0.05–0.5% Relative Standard Deviation (RSD) (Komárek et al., 2008; Andrén et al., 2004).

To address this need for higher precision, advancements in mass spectrometry technology have led to the development of Multi-Collector Inductively Coupled Plasma Mass Spectrometry (MC-ICP-MS) and Magnetic Sector Inductively Coupled Plasma Mass Spectrometry (MS-ICP-MS). The precision has been significantly improved, achieving ≥0.002% Relative Standard Deviation (RSD). Multi-collector (MC-ICP-MS) and Magnetic Sector (MS-ICP-MS) were invented later to increase the performance of precision (≥0.002%RSD). Nowadays, a great variety of ICP-based mass spectrometers are commercially available, including quadrupole-based (ICP-QMS), MC-ICP-MS, and High Resolution/MS-ICP-MS. The precision of their measurements is summarized in Table 7.

In the context of research aimed at tracing and assessing impacts of U-mining contamination, maintaining a measurement precision of

less than 0.1% for $^{206}Pb/^{207}Pb$ and $^{208}Pb/^{207}Pb$ ratios are generally adequate for differentiating U-rich materials mixed with materials from the geochemical background.

To obtain accurate and precise measurements, it is also necessary to correct the instrumental mass discrimination, using a mass discrimination factor K. Either external or internal calibration could be adopted as a correction method. The external calibration involves additional measurements of an isotopic Pb standard such as NIST SRM981 (or NIST SRM983), where the Pb isotopic ratios and the composition of the standard analyte are precisely known. On the other hand, internal calibration involves adding a standard to the sample solutions, such as the determination of the $^{203}Tl/^{205}Tl$ ratio (NIST 997—Isotopic Standard for Thallium), followed by subsequent calculation of the mass discrimination factor (Woodhead et al., 1995; Thirlwall, 2000). Concerning the spectral interference in Pb isotopic analysis, it originates mainly from isobaric elements ^{204}Hg. To mitigate this interference, the isotope ratio $^{202}Hg/^{204}Hg$ or $^{201}Hg/^{204}Hg$ serves as a method to compensate for the impact of ^{204}Hg on the ^{204}Pb (Ghazi and Millette, 2005; Hamelin et al., 1985).

5. Conclusion

This review summarized articles published on the identification of U mining contamination downstream of former U mines by using Pb stable isotopes. Even though environmental concerns such as wastewater treatment plants have been integrated into the management plans of most U-mine sites by the operators, in certain cases, mining activities have resulted in the dispersion of radioactive materials. These contaminants, along with associated heavy metals, are dispersed through hydraulic and eolian transport in both dissolved and particulate forms. Pb isotopic fingerprinting has been demonstrated as a powerful tool to accurately identify and quantify the environmental impacts of U mining activities. The uranogenic Pb enabling the differentiation of U mining sources from natural and other anthropogenic Pb sources. The successful application of this technique necessitates the characterization of potential Pb sources (endmembers), including U ores and natural Pb, and the clear differentiation of Pb isotopic compositions between these sources. The importance of a profound understanding of the mixing models they express and the choice of isotope ratio versus isotope abundances was also presented. Furthermore, the preparation and analysis of Pb isotope samples are crucial, involving digestion/extraction and measurements using ICP-MS. The combination of digestion and extraction methods can be used to understand the obtained results of Pb isotopic ratios, and accurate correction of the raw ICP-MS data is essential to ensure reliable results.

CRediT authorship contribution statement

Tingting Geng: Writing – review & editing, Writing – original draft. **Olivier Péron:** Writing – review & editing, Supervision, Funding acquisition. **Arnaud Mangeret:** Writing – review & editing, Supervision. **Gilles Montavon:** Writing – review & editing, Supervision. **Alkiviadis Gourgiotis:** Writing – review & editing, Supervision, Project administration, Conceptualization.

Declaration of competing interest

The authors declare that they have no known competing financial interests or personal relationships that could have appeared to influence the work reported in this paper.

Data availability

Data will be made available on request.

Acknowledgments

We would like to thank the Pays de la Loire doctoral grants, which have co-funded this work. The authors extend warm thanks to the reviewers for their constructive comments, which enhanced the article's quality.

References

Abdelouas, A., 2006. Uranium mill tailings: Geochemistry, mineralogy, and environmental impact. Elements 2 (6), 335–341. http://dx.doi.org/10.2113/gselements.2.6.335, URL https://pubs.geoscienceworld.org/msa/elements/article-abstract/2/6/335/137720/Uranium-Mill-Tailings-Geochemistry-Mineralogy-and. Publisher: GeoScienceWorld.

Albarède, F., Beard, B., 2004. Analytical methods for non-traditional isotopes. Rev. Mineral. Geochem. 55 (1), 113–152. http://dx.doi.org/10.2138/gsrmg.55.1.113.

Alexandre, P., Kyser, T.K., 2005. Effects of cationic substitutions and alteration in uraninite, and implications for the dating of uranium deposits. Can. Mineral. 43 (3), 1005–1017. http://dx.doi.org/10.2113/gscanmin.43.3.1005.

Andrén, H., Rodushkin, I., Stenberg, A., Malinovsky, D., Baxter, D.C., 2004. Sources of mass bias and isotope ratio variation in multi-collector ICP-MS: optimization of instrumental parameters based on experimental observations. J. Anal. At. Spectrom. 19 (9), 1217–1224. http://dx.doi.org/10.1039/B403938F, URL https://pubs.rsc.org/en/content/articlelanding/2004/ja/b403938f. Publisher: The Royal Society of Chemistry.

ASN, 2022. Le plan national de gestion des matières et déchets radioactifs. URL https://www.asn.fr/espace-professionnels/installations-nucleaires/le-plan-national-de-gestion-des-matieres-et-dechets-radioactifs.

Avasarala, S., Lichtner, P.C., Ali, A.-M.S., González-Pinzón, R., Blake, J.M., Cerrato, J.M., 2017. Reactive transport of U and V from abandoned uranium mine wastes. Environ. Sci. Technol. 51 (21), 12385–12393. http://dx.doi.org/10.1021/acs.est.7b03823, Publisher: American Chemical Society.

Beaumais, A., Mangeret, A., Suhard, D., Blanchart, P., Neji, M., Cazala, C., Gourgiotis, A., 2022. Combined U-pb isotopic signatures of u mill tailings from France and gabon: A new potential tracer to assess their fingerprint on the environment. J. Hazard. Mater. 430, 128484. http://dx.doi.org/10.1016/j.jhazmat.2022.128484, URL https://linkinghub.elsevier.com/retrieve/pii/S0304389422002722.

Berman, R.M., 1957. The Role of Lead and Excess Oxygen in Uranite. Technical Report 57–11, U.S. Geological Survey, http://dx.doi.org/10.3133/ofr5711, URL https://pubs.usgs.gov/publication/ofr5711. ISSN: 2331-1258 Publication Title: Open-File Report.

Bird, G., 2011. Provenancing anthropogenic Pb within the fluvial environment: Developments and challenges in the use of Pb isotopes. Environ. Int. 37 (4), 802–819. http://dx.doi.org/10.1016/j.envint.2011.02.007, URL https://www.sciencedirect.com/science/article/pii/S0160412011000389.

Bollhöfer, A., 2012. Stable lead isotope ratios and metals in freshwater mussels from a uranium mining environment in Australia's wet-dry tropics. Appl. Geochem. 27 (1), 171–185. http://dx.doi.org/10.1016/j.apgeochem.2011.10.002, URL https://www.sciencedirect.com/science/article/pii/S0883292711004227.

Bollhöfer, A., Honeybun, R., Rosman, K., Martin, P., 2006a. The lead isotopic composition of dust in the vicinity of a uranium mine in northern Australia and its use for radiation dose assessment. Sci. Total Environ. 366 (2), 579–589. http://dx.doi.org/10.1016/j.scitotenv.2005.11.016, URL https://www.sciencedirect.com/science/article/pii/S0048969705008430.

Bollhöfer, A., Storm, J., Martin, P., Tims, S., 2006b. Geographic variability in radon exhalation at a rehabilitated uranium mine in the northern territory, Australia. Environ. Monit. Assess. 114 (1), 313–330. http://dx.doi.org/10.1007/s10661-006-4777-z.

Burns, P.C., Finch, R.J., 2018. Uranium: Mineralogy, Geochemistry, and the Environment. Walter de Gruyter GmbH & Co KG, Google-Books-ID: CbB6DwAAQBAJ.

Cheema, A.I., Liu, G., Yousaf, B., Abbas, Q., Zhou, H., 2020. A comprehensive review of biogeochemical distribution and fractionation of lead isotopes for source tracing in distinct interactive environmental compartments. Sci. Total Environ. 719, 135658. http://dx.doi.org/10.1016/j.scitotenv.2019.135658, URL https://www.sciencedirect.com/science/article/pii/S0048969719356530.

Cheng, H., Hu, Y., 2010. Lead (pb) isotopic fingerprinting and its applications in lead pollution studies in China: A review. Environ. Pollut..

Chow, T.J., Patterson, C.C., 1962. The occurrence and significance of lead isotopes in pelagic sediments. Geochim. Cosmochim. Acta 26 (2), 263–308. http://dx.doi.org/10.1016/0016-7037(62)90016-9, URL https://www.sciencedirect.com/science/article/pii/0016703762900169.

Coetzee, H., Rademeyer, M., 2006. Lead isotope ratios as a tracer for contaminated waters from uranium mining and milling. In: Merkel, B.J., Hasche-Berger, A. (Eds.), Uranium in the Environment: Mining Impact and Consequences. Springer, Berlin, Heidelberg, pp. 663–670. http://dx.doi.org/10.1007/3-540-28367-6_67.

Cumming, G.L., Richards, J.R., 1975. Ore lead isotope ratios in a continuously changing earth. Earth Planet. Sci. Lett. 28 (2), 155–171. http://dx.doi.org/10.1016/0012-821X(75)90223-X, URL https://www.sciencedirect.com/science/article/pii/0012821X7590223X.

Cuvier, A., Panza, F., Pourcelot, L., Foissard, B., Cagnat, X., Prunier, J., van Beek, P., Souhaut, M., Le Roux, G., 2015. Uranium decay daughters from isolated mines: Accumulation and sources. J. Environ. Radioact. 149, 110–120. http://dx.doi.org/10.1016/j.jenvrad.2015.07.008, URL https://linkinghub.elsevier.com/retrieve/pii/S0265931X15300503.

Cuvier, A., Pourcelot, L., Probst, A., Prunier, J., Le Roux, G., 2016. Trace elements and Pb isotopes in soils and sediments impacted by uranium mining. Sci. Total Environ. 566–567, 238–249. http://dx.doi.org/10.1016/j.scitotenv.2016.04.213, URL https://www.sciencedirect.com/science/article/pii/S0048969716309561.

Dahlkamp, F.J., 2013. Uranium Ore Deposits. Springer Science & Business Media, Google-Books-ID: uczsCAAAQBAJ.

Dana, J.D., Klein, C., Hurlbut, C.S., 1985. Manual of Mineralogy. Wiley, Google-Books-ID: WZCcPQAACAAJ.

Dang, D.H., Wang, W., Pelletier, P., Poulain, A.J., Evans, R.D., 2018. Uranium dispersion from U tailings and mechanisms leading to U accumulation in sediments: Insights from biogeochemical and isotopic approaches. Sci. Total Environ. 610–611, 880–891. http://dx.doi.org/10.1016/j.scitotenv.2017.08.156, URL https://www.sciencedirect.com/science/article/pii/S004896971732154X.

Dickson, B.L., Gulson, B.L., Snelling, A.A., 1985. Evaluation of lead isotopic methods for uranium exploration, Koongarra Area, Northern Territory, Australia. J. Geochem. Explor. 24 (1), 81–102. http://dx.doi.org/10.1016/0375-6742(85)90005-6, URL https://www.sciencedirect.com/science/article/pii/0375674285900056.

Dickson, B.L., Gulson, B.L., Snelling, A.A., 1987. Further assessment of stable lead isotope measurements for uranium exploration, Pine Creek Geosyncline, Northern Territory, Australia. J. Geochem. Explor. 27 (1), 63–75. http://dx.doi.org/10.1016/0375-6742(87)90005-7, URL https://www.sciencedirect.com/science/article/pii/0375674287900057.

Doe, B.R., Delevaux, M.H., 1972. Source of lead in southeast missouri galena ores. Econ. Geol. 67 (4), 409–425. http://dx.doi.org/10.2113/gsecongeo.67.4.409.

Etschmann, B.E., Mei, Y., Liu, W., Sherman, D., Testemale, D., Müller, H., Rae, N., Kappen, P., Brugger, J., 2018. The role of Pb(II) complexes in hydrothermal mass transfer: An X-ray absorption spectroscopic study. Chem. Geol. 502, 88–106. http://dx.doi.org/10.1016/j.chemgeo.2018.10.022, URL https://www.sciencedirect.com/science/article/pii/S0009254118305254.

Evins, L.Z., Jensen, K.A., Ewing, R.C., 2005. Uraninite recrystallization and Pb loss in the Oklo and Bangombé natural fission reactors, Gabon. Geochim. Cosmochim. Acta 69 (6), 1589–1606. http://dx.doi.org/10.1016/j.gca.2004.07.013, URL https://www.sciencedirect.com/science/article/pii/S0016703704005666.

Fayek, M., Horita, J., Ripley, E.M., 2011. The oxygen isotopic composition of uranium minerals: A review. Ore Geol. Rev. 41 (1), 1–21. http://dx.doi.org/10.1016/j.oregeorev.2011.06.005, URL https://www.sciencedirect.com/science/article/pii/S0169136811000618.

Frostick, A., Bollhöfer, A., Parry, D., 2011. A study of radionuclides, metals and stable lead isotope ratios in sediments and soils in the vicinity of natural U-mineralisation areas in the Northern Territory. J. Environ. Radioact. 102 (10), 911–918. http://dx.doi.org/10.1016/j.jenvrad.2010.04.003, URL https://www.sciencedirect.com/science/article/pii/S0265931X1000086X.

Frostick, A., Bollhöfer, A., Parry, D., Munksgaard, N., Evans, K., 2008. Radioactive and radiogenic isotopes in sediments from Cooper Creek, Western Arnhem Land. J. Environ. Radioact. 99 (3), 468–482. http://dx.doi.org/10.1016/j.jenvrad.2007.08.015, URL https://www.sciencedirect.com/science/article/pii/S0265931X07002263.

Geng, T., Mangeret, A., Péron, O., Suhard, D., Gorny, J., Darricau, L., Le Coz, M., Ait-ouabbas, N., David, K., Debayle, C., Blanchart, P., Montavon, G., Gourgiotis, A., 2024. Unveiling the origins and transport processes of radioactive pollutants downstream from a former U-mine site using isotopic tracers and U-238 series disequilibrium. J. Hazard. Mater. 472, 134416. http://dx.doi.org/10.1016/j.jhazmat.2024.134416, URL https://www.sciencedirect.com/science/article/pii/S0304389424009956.

Ghazi, A.M., Millette, J.R., 2005. 4 - lead. In: Morrison, R.D., Murphy, B.L. (Eds.), Environmental Forensics. Academic Press, Burlington, pp. 55–79. http://dx.doi.org/10.1016/B978-012507751-4/50026-4, URL https://www.sciencedirect.com/science/article/pii/B9780125077514500264.

Gourgiotis, A., Mangeret, A., Manhès, G., Blanchart, P., Stetten, L., Morin, G., Le Pape, P., Lefebvre, P., Le Coz, M., Cazala, C., 2020. New insights into Pb isotope fingerprinting of U-mine material dissemination in the environment: Pb isotopes as a memory dissemination tracer. Environ. Sci. Technol. 54 (2), 797–806. http://dx.doi.org/10.1021/acs.est.9b04828, Publisher: American Chemical Society.

Gulson, B.L., Mizon, K.J., Korsch, M.J., Noller, B.N., 1989. Lead isotopes as seepage indicators around a uranium tailings dam. Environ. Sci. Technol. 23 (3), 290–294. http://dx.doi.org/10.1021/es00180a004, Publisher: American Chemical Society.

Hamelin, B., Manhes, G., Albarede, F., Allègre, C.J., 1985. Precise lead isotope measurements by the double spike technique: A reconsideration. Geochim. Cosmochim. Acta 49 (1), 173–182. http://dx.doi.org/10.1016/0016-7037(85)90202-9, URL https://www.sciencedirect.com/science/article/pii/0016703785902029.

Hills, J.H., Richards, J.R., 1976. Pitchblende and galena ages in the Alligator Rivers region, Northern Territory, Australia. Miner. Depos. 11 (2), 133–154. http://dx.doi.org/10.1007/BF00204477.

Hopper, J.F., Ross, H.B., And, 1991. Regional source discrimination of atmospheric aerosols in Europe using the isotopic composition of lead. Tellus B 43 (1), 45–60. http://dx.doi.org/10.1034/j.1600-0889.1991.00004.x, URL https://onlinelibrary.wiley.com/doi/abs/10.1034/j.1600-0889.1991.00004.x._eprint: https://onlinelibrary.wiley.com/doi/pdf/10.1034/j.1600-0889.1991.00004.x.

IRSN Mimausa, 2023. Mimausa web. URL https://mimausabdd.irsn.fr/.

Isobe, H., Hidaka, H., Ohnuki, T., 1997. SIMS analysis of lead isotopes in the primary ore body of the koongarra deposit, Australia: Behavior of lead in the alteration of uranium minerals. MRS Online Proc. Libr. (OPL) 506, 687. http://dx.doi.org/10.1557/PROC-506-687, URL https://www.cambridge.org/core/journals/mrs-online-proceedings-library-archive/article/abs/sims-analysis-of-lead-isotopes-in-the-primary-ore-body-of-the-koongarra-deposit-australia-behavior-of-lead-in-the-alteration-of-uranium-minerals/26632ACF480283FE7D1E39FCA1B7F8FD#access-block. Publisher: Cambridge University Press.

Janeczek, J., Ewing, R.C., 1991. X-ray powder diffraction study of annealed uraninite. J. Nucl. Mater. 185 (1), 66–77. http://dx.doi.org/10.1016/0022-3115(91)90366-F, URL https://www.sciencedirect.com/science/article/pii/002231159190366F.

Janeczek, J., Ewing, R.C., 1992. Structural formula of uraninite. J. Nucl. Mater. 190, 128–132. http://dx.doi.org/10.1016/0022-3115(92)90082-V, URL https://www.sciencedirect.com/science/article/pii/002231159290082V.

Janeczek, J., Ewing, R.C., 1995. Mechanisms of lead release from uraninite in the natural fission reactors in Gabon. Geochim. Cosmochim. Acta 59 (10), 1917–1931. http://dx.doi.org/10.1016/0016-7037(95)00117-4, URL https://www.sciencedirect.com/science/article/pii/0016703795001174.

Janeczek, J., Ewing, R.C., Oversby, V.M., Werme, L.O., 1996. Uraninite and UO2 in spent nuclear fuel: a comparison. J. Nucl. Mater. 238 (1), 121–130. http://dx.doi.org/10.1016/S0022-3115(96)00345-5, URL https://www.sciencedirect.com/science/article/pii/S0022311596003455.

Kamber, B.S., Gladu, A.H., 2009. Comparison of Pb purification by anion-exchange resin methods and assessment of long-term reproducibility of Th/U/Pb ratio measurements by quadrupole ICP-MS. Geostand. Geoanal. Res. 33 (2), 169–181. http://dx.doi.org/10.1111/j.1751-908X.2009.00911.x, URL https://onlinelibrary.wiley.com/doi/abs/10.1111/j.1751-908X.2009.00911.x.

Keegan, E., Richter, S., Kelly, I., Wong, H., Gadd, P., Kuehn, H., Alonso-Munoz, A., 2008. The provenance of Australian uranium ore concentrates by elemental and isotopic analysis. Appl. Geochem. 23 (4), 765–777. http://dx.doi.org/10.1016/j.apgeochem.2007.12.004, URL https://www.sciencedirect.com/science/article/pii/S0883292707003332.

Kirkland, C.L., Fougerouse, D., Reddy, S.M., Hollis, J., Saxey, D.W., 2018. Assessing the mechanisms of common Pb incorporation into titanite. Chem. Geol. 483, 558–566. http://dx.doi.org/10.1016/j.chemgeo.2018.03.026, URL https://www.sciencedirect.com/science/article/pii/S0009254118301396.

Kister, P., Cuney, M., Golubev, V.N., Royer, J.-J., Le Carlier De Veslud, C., Rippert, J.-C., 2004. Radiogenic lead mobility in the Shea Creek unconformity-related uranium deposit (Saskatchewan, Canada): migration pathways and Pb loss quantification. C. R. Geosci. 336 (3), 205–215. http://dx.doi.org/10.1016/j.crte.2003.11.006, URL https://www.sciencedirect.com/science/article/pii/S1631071303002773.

Kogawa, M., Watson, E.B., Ewing, R.C., Utsunomiya, S., 2012. Lead in zircon at the atomic scale. Am. Mineral. 97 (7), 1094–1102. http://dx.doi.org/10.2138/am.2012.3993.

Koide, Y., Nakamura, E., 1990. Lead isotope analyses of standard rock samples. J. Mass Spectrom. Soc. Japan 38 (5), 241–252. http://dx.doi.org/10.5702/massspec.38.241.

Komárek, M., Chrastný, V., Ettler, V., Tlustoš, P., 2006. Evaluation of extraction/digestion techniques used to determine lead isotopic composition in forest soils. Anal. Bioanal. Chem. 385 (6), 1109–1115. http://dx.doi.org/10.1007/s00216-006-0543-x.

Komárek, M., Ettler, V., Chrastný, V., Mihaljevič, M., 2008. Lead isotopes in environmental sciences: A review. Environ. Int. 34 (4), 562–577. http://dx.doi.org/10.1016/j.envint.2007.10.005, URL https://linkinghub.elsevier.com/retrieve/pii/S0160412007001985.

Kuritani, T., Nakamura, E., 2002. Precise isotope analysis of nanogram-level Pb for natural rock samples without use of double spikes. Chem. Geol. 186 (1), 31–43. http://dx.doi.org/10.1016/S0009-2541(02)00004-9, URL https://www.sciencedirect.com/science/article/pii/S0009254102000049.

Kusiak, M.A., Dunkley, D.J., Wirth, R., Whitehouse, M.J., Wilde, S.A., Marquardt, K., 2015. Metallic lead nanospheres discovered in ancient zircons. Proc. Natl. Acad. Sci. 112 (16), 4958–4963. http://dx.doi.org/10.1073/pnas.1415264112, URL https://www.pnas.org/doi/abs/10.1073/pnas.1415264112. Publisher: Proceedings of the National Academy of Sciences.

Langmuir, D., 1978. Uranium solution-mineral equilibria at low temperatures with applications to sedimentary ore deposits. Geochim. Cosmochim. Acta 42 (6, Part A), 547–569. http://dx.doi.org/10.1016/0016-7037(78)90001-7, URL https://www.sciencedirect.com/science/article/pii/0016703778900017.

Lefebvre, P., Le Pape, P., Mangeret, A., Gourgiotis, A., Sabatier, P., Louvat, P., Diez, O., Mathon, O., Hunault, M.O.J.Y., Baya, C., Darricau, L., Cazala, C., Bargar, J.R., Gaillardet, J., Morin, G., 2022. Uranium sorption to organic matter and long-term accumulation in a pristine alpine wetland. Geochim. Cosmochim. Acta 338, 322–346. http://dx.doi.org/10.1016/j.gca.2022.10.018, URL https://www.sciencedirect.com/science/article/pii/S0016703722005579.

Lévêque, M.-H., 1990. Contribution de la Géochronologie U-Pb à la Caractérisation du Magmatisme Cadomien de la Partie Sud-Est du Massif Central et du Gisement d'Uranium Associé de Bertholène (Ph.D. thesis). Montpellier 2, URL https://www.theses.fr/1990MON20080.

Liu, J., Luo, X., Wang, J., Xiao, T., Yin, M., Belshaw, N.S., Lippold, H., Kong, L., Xiao, E., Bao, Z., Li, N., Chen, Y., Linghu, W., 2018. Provenance of uranium in a sediment core from a natural reservoir, south China: Application of Pb stable isotope analysis. Chemosphere 193, 1172–1180. http://dx.doi.org/10.1016/j.chemosphere.2017.11.131, URL https://www.sciencedirect.com/science/article/pii/S0045653517319082.

MacMillan, E.I., 2016. The evolution of uraninite, coffinite and brannerite from the olympic dam iron oxide-copper-gold-silveruranium deposit: linking textural observations to compositional variability. http://dx.doi.org/10.4225/55/59a61fde17204, URL https://digital.library.adelaide.edu.au/dspace/handle/2440/107374. Accepted: 2017-08-30T02:36:19Z.

Mangeret, A., Blanchart, P., Alcalde, G., Amet, X., Cazala, C., Gallerand, M.-O., 2018. An evidence of chemically and physically mediated migration of 238u and its daughter isotopes in the vicinity of a former uranium mine. J. Environ. Radioact. 195, 67–71. http://dx.doi.org/10.1016/j.jenvrad.2018.08.018, URL https://www.sciencedirect.com/science/article/pii/S0265931X17310007.

Mangeret, A., Reyss, J.-L., Seder-Colomina, M., Stetten, L., Morin, G., Thouvenot, A., Souhaut, M., van Beek, P., 2020. Early diagenesis of radium 226 and radium 228 in lacustrine sediments influenced by former mining sites. J. Environ. Radioact. 222, 106324. http://dx.doi.org/10.1016/j.jenvrad.2020.106324, URL https://www.sciencedirect.com/science/article/pii/S0265931X19310203.

Manhes, G., Allegre, C.J., Provost, A., 1984. U-Th-Pb systematics of the eucrite "Juvinas": Precise age determination and evidence for exotic lead. Geochim. Cosmochim. Acta 48 (11), 2247–2264. http://dx.doi.org/10.1016/0016-7037(84)90221-7, URL https://www.sciencedirect.com/science/article/pii/0016703784902217.

Martin, A., Hassan-Loni, Y., Fichtner, A., Péron, O., David, K., Chardon, P., Larrue, S., Gourgiotis, A., Sachs, S., Arnold, T., Grambow, B., Stumpf, T., Montavon, G., 2020. An integrated approach combining soil profile, records and tree ring analysis to identify the origin of environmental contamination in a former uranium mine (Rophin, France). Sci. Total Environ. 747, 141295. http://dx.doi.org/10.1016/j.scitotenv.2020.141295, URL https://www.sciencedirect.com/science/article/pii/S0048969720348245.

Martin, A., Montavon, G., Landesman, C., 2021. A combined DGT - DET approach for an in situ investigation of uranium resupply from large soil profiles in a wetland impacted by former mining activities. Chemosphere 279, 130526. http://dx.doi.org/10.1016/j.chemosphere.2021.130526, URL https://www.sciencedirect.com/science/article/pii/S0045653521009978.

Millet, M.-A., 2007. Interactions de Faibles Profondeurs et Géochimie des Basaltes D'îles Océaniques: Implications sur les Modes d'Acquisition de la Signature Isotopique et sur la Topogique Mantellique (Ph.D. thesis). Université Blaise Pascal - Clermont-Ferrand II, URL https://theses.hal.science/tel-00718419.

Monna, F., Aiuppa, A., Varrica, D., Dongarra, G., 1999. Pb isotope composition in lichens and aerosols from eastern sicily: Insights into the regional impact of volcanoes on the environment. Environ. Sci. Technol. 33 (15), 2517–2523. http://dx.doi.org/10.1021/es9812251, Publisher: American Chemical Society.

Monna, F., Lancelot, J., Croudace, I.W., Cundy, A.B., Lewis, J.T., 1997. Pb isotopic composition of airborne particulate material from France and the southern United Kingdom: Implications for Pb pollution sources in urban areas. Environ. Sci. Technol. 31 (8), 2277–2286. http://dx.doi.org/10.1021/es960870+.

Morin, G., Mangeret, A., Othmane, G., Stetten, L., Seder-Colomina, M., Brest, J., Ona-Nguema, G., Bassot, S., Courbet, C., Guillevic, J., Antoine, T., Mathon, O., Proux, O., Bargar, J., 2016. Mononuclear U(IV) complexes and ningyoite as major uranium species in lake sediments. Geochem. Persp. Lett. 2, http://dx.doi.org/10.7185/geochemlet.1610.

Munksgaard, N.C., Brazier, J.A., Moir, C.M., Parry, D.L., 2003. The use of lead isotopes in monitoring environmental impacts of uranium and lead mining in northern Australia. Aust. J. Chem. 56 (3), 233–238. http://dx.doi.org/10.1071/ch02239, URL https://www.publish.csiro.au/ch/ch02239. Publisher: CSIRO PUBLISHING.

Owen, D.E., Otton, J.K., 1995. Mountain wetlands: Efficient uranium filters — potential impacts. Ecol. Eng. 5 (1), 77–93. http://dx.doi.org/10.1016/0925-8574(95)00013-9, URL https://www.sciencedirect.com/science/article/pii/0925857495000139.

Peña, J., Straub, M., Flury, V., Loup, E., Corcho, J., Steinmann, P., Bochud, F., Froidevaux, P., 2020. Origin and stability of uranium accumulation-layers in an Alpine histosol. Sci. Total Environ. 727, 138368. http://dx.doi.org/10.1016/j.scitotenv.2020.138368, URL https://www.sciencedirect.com/science/article/pii/S0048969720318817.

Pomiès, C., Hamelin, B., Lancelot, J., Blomqvist, R., 2004. 207Pb/206Pb and 238U/230Th dating of uranium migration in carbonate fractures from the Palmottu uranium ore (southern Finland). Appl. Geochem. 19 (3), 273–288. http://dx.doi.org/10.1016/S0883-2927(03)00134-3, URL https://www.sciencedirect.com/science/article/pii/S0883292703001343.

Quétel, C.R., Thomas, B., Donard, O.F.X., Grousset, F.E., 1997. Factorial optimization of data acquisition factors for lead isotope ratio determination by inductively coupled plasma mass spectrometry. Spectrochim. Acta B Atom. Spectrosc. 52 (2), 177–187. http://dx.doi.org/10.1016/S0584-8547(96)01587-X, URL https://www.sciencedirect.com/science/article/pii/S058485479601587X.

Quirt, D., Benedicto, A., 2020. Lead isotopes in exploration for basement-hosted structurally controlled unconformity-related uranium deposits: Kiggavik project (Nunavut, Canada). Minerals 10 (6), 512. http://dx.doi.org/10.3390/min10060512, URL https://www.mdpi.com/2075-163X/10/6/512. Number: 6 Publisher: Multidisciplinary Digital Publishing Institute.

Ram, R., Morrisroe, L., Etschmann, B., Vaughan, J., Brugger, J., 2021. Lead (Pb) sorption and co-precipitation on natural sulfide, sulfate and oxide minerals under environmental conditions. Miner. Eng. 163, 106801. http://dx.doi.org/10.1016/j.mineng.2021.106801, URL https://www.sciencedirect.com/science/article/pii/S0892687521000303.

Regenspurg, S., Margot-Roquier, C., Harfouche, M., Froidevaux, P., Steinmann, P., Junier, P., Bernier-Latmani, R., 2010. Speciation of naturally-accumulated uranium in an organic-rich soil of an alpine region (Switzerland). Geochim. Cosmochim. Acta 74 (7), 2082–2098. http://dx.doi.org/10.1016/j.gca.2010.01.007, URL https://www.sciencedirect.com/science/article/pii/S0016703710000165.

Rollog, M., Cook, N.J., Guagliardo, P., Ehrig, K.J., Kilburn, M., 2019. Radionuclide-bearing minerals in Olympic Dam copper concentrates. Hydrometallurgy 190, 105153. http://dx.doi.org/10.1016/j.hydromet.2019.105153, URL https://www.sciencedirect.com/science/article/pii/S0304386X19304232.

Rossman, G., 1972. Use of radiogenic Pb206 halos in prospecting for uranium in acidic volcanic rocks. Int. Geol. Rev. 14 (4), 332–337. http://dx.doi.org/10.1080/00206817209475702, Publisher: Taylor & Francis _eprint: https://doi.org/10.1080/00206817209475702.

Sangster, D.F., Outridge, P.M., Davis, W.J., 2000. Stable lead isotope characteristics of lead ore deposits of environmental significance. Environ. Rev. 8 (2), 115–147. http://dx.doi.org/10.1139/a00-008, URL https://cdnsciencepub.com/doi/abs/10.1139/a00-008. Publisher: NRC Research Press.

Santos, R.M., Tassinari, C.C.G., 2012. Different lead sources in an abandoned uranium mine (Urgeiriça - Central Portugal) and its environment impact – isotopic evidence. Geochem. Explor. Environ. Anal. 12 (3), 241–252. http://dx.doi.org/10.1144/1467-7873/11-RA-076, URL https://www.lyellcollection.org/doi/10.1144/1467-7873/11-RA-076. Publisher: The Geological Society of London.

Stacey, J.S., Kramers, J.D., 1975. Approximation of terrestrial lead isotope evolution by a two-stage model. Earth Planet. Sci. Lett. 26 (2), 207–221. http://dx.doi.org/10.1016/0012-821X(75)90088-6, URL https://www.sciencedirect.com/science/article/pii/0012821X75900886.

Stetten, L., 2018. Spéciation et Mobilité de l'Uranium dans des Sols et des Sédiments Lacustres en Aval d'Anciens Sites Miniers (Ph.D. thesis). Sorbonne Université, URL https://theses.hal.science/tel-02475854.

Stetten, L., Blanchart, P., Mangeret, A., Lefebvre, P., Le Pape, P., Brest, J., Merrot, P., Julien, A., Proux, O., Webb, S.M., Bargar, J.R., Cazala, C., Morin, G., 2018. Redox fluctuations and organic complexation govern uranium redistribution from U(IV)-phosphate minerals in a mining-polluted wetland soil, Brittany, France. Environ. Sci. Technol. 52 (22), 13099–13109. http://dx.doi.org/10.1021/acs.est.8b03031, URL https://pubs.acs.org/doi/10.1021/acs.est.8b03031.

Švedkauskaite-LeGore, J., Mayer, K., Millet, S., Nicholl, A., Rasmussen, G., Baltrunas, D., 2007. Investigation of the isotopic composition of lead and of trace elements concentrations in natural uranium materials as a signature in nuclear forensics. Radiochim. Acta 95 (10), 601–605. http://dx.doi.org/10.1524/ract.2007.95.10.601, URL https://www.degruyter.com/document/doi/10.1524/ract.2007.95.10.601/html. Publisher: De Gruyter (O).

Syverson, D.D., Etschmann, B., Liu, W., Ram, R., Mei, Y., Lanzirotti, T., Mercadier, J., Brugger, J., 2019. Oxidation state and coordination environment of Pb in U-bearing minerals. Geochim. Cosmochim. Acta 265, 109–131. http://dx.doi.org/10.1016/j.gca.2019.08.039, URL https://www.sciencedirect.com/science/article/pii/S0016703719305605.

Tanimizu, M., Ishikawa, T., 2006. Development of rapid and precise Pb isotope analytical techniques using MC-ICP-MS and new results for GSJ rock reference samples. Geochem. J. 40 (2), 121–133. http://dx.doi.org/10.2343/geochemj.40.121.

Tatsumoto, M., Knight, R.J., Allegre, C.J., 1973. Time differences in the formation of meteorites as determined from the ratio of lead-207 to lead-206. Science 180 (4092), 1279–1283. http://dx.doi.org/10.1126/science.180.4092.1279, URL https://www.science.org/doi/abs/10.1126/science.180.4092.1279.

Thirlwall, M.F., 2000. Inter-laboratory and other errors in Pb isotope analyses investigated using a 207Pb–204Pb double spike. Chem. Geol. 163 (1), 299–322. http://dx.doi.org/10.1016/S0009-2541(99)00135-7, URL https://www.sciencedirect.com/science/article/pii/S0009254199001357.

Varga, Z., Wallenius, M., Mayer, K., Keegan, E., Millet, S., 2009. Application of lead and strontium isotope ratio measurements for the origin assessment of uranium ore concentrates. Anal. Chem. 81 (20), 8327–8334. http://dx.doi.org/10.1021/ac901100e, Publisher: American Chemical Society.

Vecchia, A.M.D., Rodrigues, P.C.H., Rios, F.J., Ladeira, A.C.Q., 2017. Investigations into Pb isotope signatures in groundwater and sediments in a uranium-mineralized area. Braz. J. Geol. 47, 147–158. http://dx.doi.org/10.1590/2317-4889201720160100, URL http://www.scielo.br/j/bjgeo/a/4gK7Y4DdSYQXjHPxvvh6bZf/?lang=en. Publisher: Sociedade Brasileira de Geologia.

Wang, Y., Bagnoud, A., Suvorova, E., McGivney, E., Chesaux, L., Phrommavanh, V., Descostes, M., Bernier-Latmani, R., 2014. Geochemical control on uranium(IV) mobility in a mining-impacted wetland. Environ. Sci. Technol. 48 (17), 10062–10070. http://dx.doi.org/10.1021/es501556d, Publisher: American Chemical Society.

Wang, Y., Frutschi, M., Suvorova, E., Phrommavanh, V., Descostes, M., Osman, A.A.A., Geipel, G., Bernier-Latmani, R., 2013. Mobile uranium(IV)-bearing colloids in a mining-impacted wetland. Nature Commun. 4 (1), 2942. http://dx.doi.org/10.1038/ncomms3942, URL https://www.nature.com/articles/ncomms3942. Number: 1 Publisher: Nature Publishing Group.

Wang, J., Hu, H., Lin, K., Wei, X., Beiyuan, J., Xiong, X., Wan, Y., Deng, P., Wu, H., Kang, M., Liu, J., Dong, X., 2024. Pb isotopic fingerprinting of uranium pollution: New insight on uranium transport in stream-river sediments. J. Hazard. Mater. 472, 134417. http://dx.doi.org/10.1016/j.jhazmat.2024.134417, URL https://www.sciencedirect.com/science/article/pii/S0304389424009968.

Watson, E.B., Chemiak, D.J., Hanchar, J.M., Harrison, T.M., Wark, D.A., 1997. The incorporation of Pb into zircon. Chem. Geol. 141 (1), 19–31. http://dx.doi.org/10.1016/S0009-2541(97)00054-5, URL https://www.sciencedirect.com/science/article/pii/S0009254197000545.

Weiss, D., Shotyk, W., Kramers, J.D., Gloor, M., 1999. *Sphagnum* mosses as archives of recent and past atmospheric lead deposition in Switzerland. Atmos. Environ. 33 (23), 3751–3763. http://dx.doi.org/10.1016/S1352-2310(99)00093-X, URL https://www.sciencedirect.com/science/article/pii/S135223109900093X.

Woodhead, J.D., Volker, F., McCulloch, M.T., 1995. Routine lead isotope determinations using a lead-207–lead-204 double spike: a long-term assessment of analytical precision and accuracy. Analyst 120 (1), 35–39. http://dx.doi.org/10.1039/AN9952000035, URL https://pubs.rsc.org/en/content/articlelanding/1995/an/an9952000035. Publisher: The Royal Society of Chemistry.